Pergamon

Cement and Concrete Research 30 (2000) 953–962

CEMENT AND CONCRETE RESEARCH

Influence of silica fume on diffusivity in cement-based materials I. Experimental and computer modeling studies on cement pastes

D.P. Bentz[a,*], O.M. Jensen[b], A.M. Coats[c], F.P. Glasser[c]

[a]*Building and Fire Research Laboratory, National Institute of Standards and Technology, 100 Bureau Drive Stop 8621, Gaithersburg, MD 20899-8621 USA*
[b]*Institute of Building Technology and Structural Engineering, Aalborg University, Alborg, Denmark*
[c]*Department of Chemistry, University of Aberdeen, Aberdeen, Scotland, UK*

Received 20 October 1999; accepted 22 March 2000

Abstract

Experimental and computer modeling studies are applied in determining the influence of silica fume on the microstructure and diffusivity of cement paste. It is suggested that silica fume modifies the inherent nanostructure of the calcium silicate hydrate (C-S-H) gel, reducing its porosity and thus increasing its resistance to diffusion of both tritiated water and chloride ions. Because the pores in the C-S-H are extremely fine, the relative reduction in diffusion depends on the specific diffusing species. Based on the NIST cement hydration and microstructural model, for tritiated water diffusion, the reduction in the diffusivity of the gel caused by silica fume is about a factor of five. For chloride ions, when a diffusivity value 25 times lower than that used for conventional high Ca/Si ratio C-S-H is assigned to the pozzolanic lower Ca/Si ratio C-S-H, excellent agreement is obtained between experimental chloride ion diffusivity data and results generated based on the NIST model, for silica fume additions ranging from 0% to 10%. For higher addition rates, the experimentally observed reduction in diffusivity is significantly greater than that predicted from the computer models, suggesting that at these very high dosages, the nanostructure of the pozzolanic C-S-H may be even further modified. Based on the hydration model, a percolation-based explanation of the influence of silica fume on diffusivity is proposed and a set of equations relating diffusivity to capillary porosity and silica fume addition rate is developed. A 10% addition of silica fume may result in a factor of 15 or more reduction in chloride ion diffusion and could potentially lead to a substantial increase in the service life of steel-reinforced concrete exposed to a severe environment.

Keywords: Cement paste; Diffusion; Hydration; Modeling; Silica fume

1. Introduction

The engineering of more durable concrete has been a major goal of the 1990s. Reducing the water-to-cement (w/c) ratio significantly below 0.4 has resulted in the production of dense concretes with very little water-filled capillary porosity. In these high-performance concretes, some empty capillary porosity will be generated due to the chemical shrinkage and self-desiccation that occurs during cement hydration [1,2]. For the most part, their transport properties will be dominated by two criteria: the volume fraction, width, and percolation of cracks, and the transport properties of the nanoporous calcium silicate hydrate (C-S-H) gel. By careful attention to mixture proportions and curing conditions, cracking can be avoided or at least minimized. This implies that further advances in increasing the durability of concrete may be obtained by engineering the nanostructure of the C-S-H, as has been proposed previously [3].

The ability of silica fume to reduce the diffusivity and permeability of concrete is well documented [4–6], but still controversial. The center of the controversy results from the prevalent usage of the rapid chloride permeability test (RCPT) to assess the resistance of concrete to chloride ion diffusion [7]. Unfortunately, a reduction in the RCPT-measured value can be due to several factors, including a change in the conductivity of the pore solution as well as a "real" change in the pore volume and tortuosity. Silica fume (CSF) affects both the pore structure and the $[OH^-]$ concentration of the pore solution [6], so a clear delineation of its effects is still somewhat lacking. Recently, Jensen et al. [8] have

* Corresponding author: Tel.: +1-301-975-5865; fax: +1-301-990-6891.
E-mail address: dale.bentz@nist.gov (D.P. Bentz).

0008-8846/00/$ – see front matter
PII: S0008-8846(00)00264-7

Table 1
Bogue potential phase composition of cement

Phase	Mass %
C_3S	66.1
C_2S	21.2
C_3A	4.3
C_4AF	1.1
$C\bar{S}$	3.5
Free CaO	1.96
Na_2O equivalent	0.17

performed a series of high resolution electron probe microanalysis (EPMA) measurements to directly determine the effects of silica fume addition on the penetration of chloride ions into cement pastes. In this paper, the NIST cement hydration and microstructural development model will be used to interpret the experimental measurements and develop a more consistent view of the mechanisms by which silica fume reduces the diffusivity of cement-based materials.

2. Structure of the pozzolanic C-S-H gel

To correctly model the influence of silica fume on cement paste diffusivity, one must begin with the nanostructure of the C-S-H. Only when an appropriate value(s) is used for the diffusivity of the gel can the cement paste diffusivity be predicted accurately. It has been known for many years that the pozzolanic C-S-H formed from the reaction of silica fume and calcium hydroxide (CH) has a different Ca/Si molar ratio and a different water content than the gel formed from conventional cement hydration [9–11]. However, until recently, the question remained open as to whether the underlying nanostructure of the pozzolanic C-S-H differed from that of conventional C-S-H. Based on a series of adsorption/desorption measurements on cement pastes with 10% and without silica fume, Baroghel-Bouny [12] has deduced that the pozzolanic C-S-H has a porosity of only 19%, in comparison with the value of 28% for the conventional C-S-H estimated by Powers and Brownyard [13,14].

Previously, a two-level structural model for the C-S-H has been developed based on partially overlapping spheres [15]. At the macro level, the model consists of partially overlapping spheres 40 nm in overall diameter, with an interparticle porosity of 7.6%. The remainder of the 28% porosity is present at the micro level, where the model consists of partially overlapping spheres 5 nm in diameter, in accordance with small angle neutron scattering measurements [16]. For the macro level, based on an electrical analogy [15], a formation factor of about 230 is computed. Here, the formation factor is defined as the ratio of the diffusivity of an ion in bulk water to that in the water-filled porous composite material. This value of 230 compares reasonably well with a value of 400 used previously to provide agreement between cement hydration model and experimental diffusivity data [17]. If one maintains the

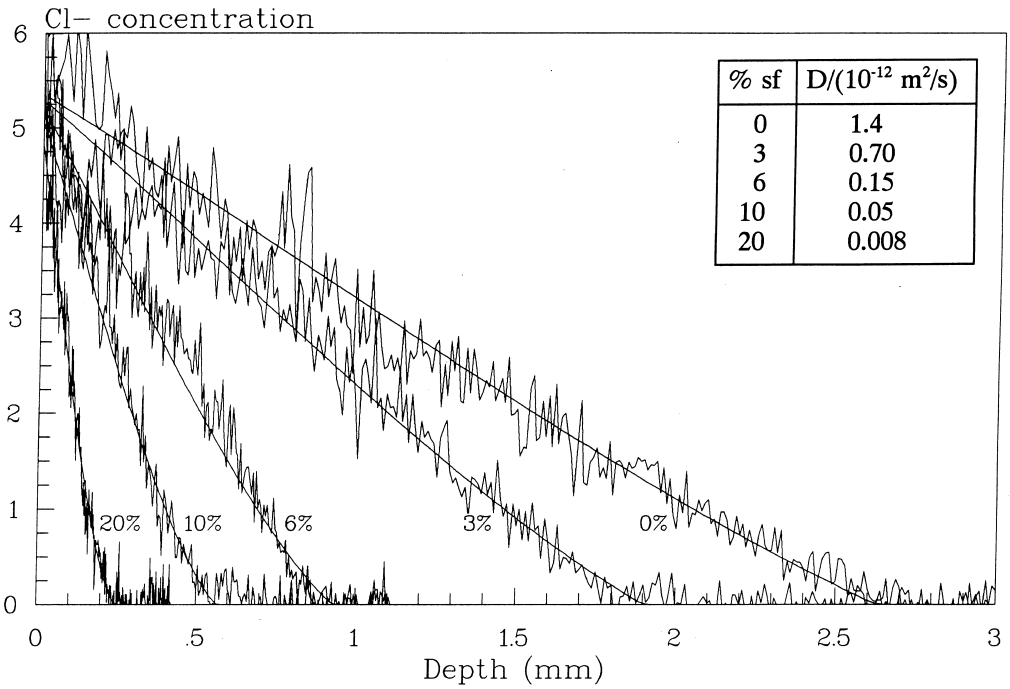

Fig. 1. Influence of silica fume addition on chloride ingress. Chloride profiles for five different pastes are shown. Except for silica fume addition, marked on the curves, the pastes are identical. The pastes have a w/c ratio (mass basis) of 0.3 and have been exposed to a 3% NaCl solution for 1 month at 20°C. Leaching was minimized throughout the chloride exposure. The smooth curves are calculated profiles with diffusion coefficients as given in the table inset within the plot. The fluctuating curves are based on the EPMA mapping [22].

Table 2
Reaction of silica fume with Portland cement

% SF 0%	Global model 20–25% CH	Local model 20–25% CH
Increasing up to about 15% to 20%	CH declines. C-S-H Ca/Si ratio remains at 1.7.	CH reaction is quantitatively less than theoretical, locally. Some C-S-H has Ca/Si ratio less than 1.7 but some high ratio material persists.
15% to 20%	All CH gone. C-S-H Ca/Si ratio is 1.7.	A few % CH persists. C-S-H has variable Ca/Si ratio but mean value is <1.7.
>15% to 20%	All CH gone. Ca/Si ratio of C-S-H decreases.	A little CH persists. Ca/Si ratio of C-S-H decreased but considerable "spread" of ratios occurs locally within material.

sphere diameter at 40 nm, but decreases the porosity to about 5.1% (5.1 = 7.6 × 19/28), the model formation factor increases to about 1080, approximately a factor of five times higher than the original gel value. A more direct and quantitative elucidation of the differences in nanostructure between the pozzolanic and conventional C-S-H may be possible in the future using either NMR spectroscopy [18,19] or low temperature calorimetry [19].

3. Materials and experimental methods

A full description of the sample preparation, measuring technique, and method for calculation of the diffusion coefficients for the cement pastes is given elsewhere [8,22]. Only a brief description is given here.

The cement used was a white Portland cement with a Blaine fineness of 420 m^2/kg, whose Bogue calculated potential phase composition is provided in Table 1. Silica fume was added as a dry powder. The silica fume employed in these experiments had a specific surface of 20.5 m^2/g and a chemical composition of (mass fraction, %): SiO_2: 90.8, Fe_2O_3: 0.94, Al_2O_3: 0.54, MgO: 1.32, and SO_3: 0.57. Superplasticizer was added at a rate of 1.0% by mass of cement + silica fume. The superplasticizer was a napthalene-based dry powder. Demineralized, freshly boiled water was used for all mixes.

Mixing was performed for 5 min in a 5 l epicyclic laboratory mixer. The water was added in two steps during mixing. This procedure ensures the homogeneity of the paste and the proper dispersion of the silica fume.

After mixing, cylindrical samples 44 mm in diameter and 21 mm in length were cast from the cement paste. These samples were then stored in lime-saturated water for approximately 100 days for prehardening and water saturation. Before the chloride exposure, approximately 1 mm was ground off of each sample base. The bottom and cylindrical surfaces of the sample were then sealed with a 1-mm layer of polyurethane, with the newly ground surface being subsequently exposed to chlorides. For this, the samples were exposed to a simulated pore solution also containing 3% NaCl (as in typical seawater) for 1 month at 20°C. In this way, leaching of the cement pastes during the chloride exposure was avoided. Leaching can have a serious influence on the ingress of chlorides, with calculated diffusion coefficients being up to 2.5 times greater under leaching than under non-leaching conditions [22].

After chloride exposure, the samples were vacuum dried and the chloride profiles were measured by EPMA. Detailed studies of various drying regimes have indicated that the chloride profiles are unaffected by the vacuum drying process [22]. Typical profiles are provided in Fig. 1. The modeled chloride profiles have been calculated with a computer program that assumes chloride transport to follow Fick's law and takes into account chloride binding by the cement paste components [8,22].

4. Computer modeling of cement paste microstructure

The NIST three-dimensional (3-D) cement hydration and microstructure development model has been described in detail previously [1]. For this study, initial 3-D cement

Table 3
Data for tritiated water diffusion in cement pastes

w/c [Ref.]	% CSF replacement	Exp. $D \times 10^{-12}$ m^2/s	Model $D \times 10^{-12}$ m^2/s
0.45 [20]	0	9.9	7.8 ± 0.3[a]
0.45 [20]	6	3.8	1.98 ± 0.02
0.25 [20]	0	0.63	0.76 ± 0.01
0.25 [20]	6	0.16	0.338 ± 0.002
0.20 [23]	0	2.0	1.11 ± 0.01

[a] SD for model diffusivity computed in each of the three principal directions.

Table 4
Data for chloride ion diffusion in w/c = 0.3 cement pastes

% CSF addition	Exp. $D \times 10^{-12}$ m^2/s	Model $D \times 10^{-12}$ m^2/s
0	1.4	1.44 ± 0.01[a]
3	0.7	0.80 ± 0.01
6	0.15	0.182 ± 0.001
10	0.05	0.0805 ± 0.0005
20	0.008	0.0769 ± 0.0002

[a] SD for model diffusivity computed in each of the three principal directions.

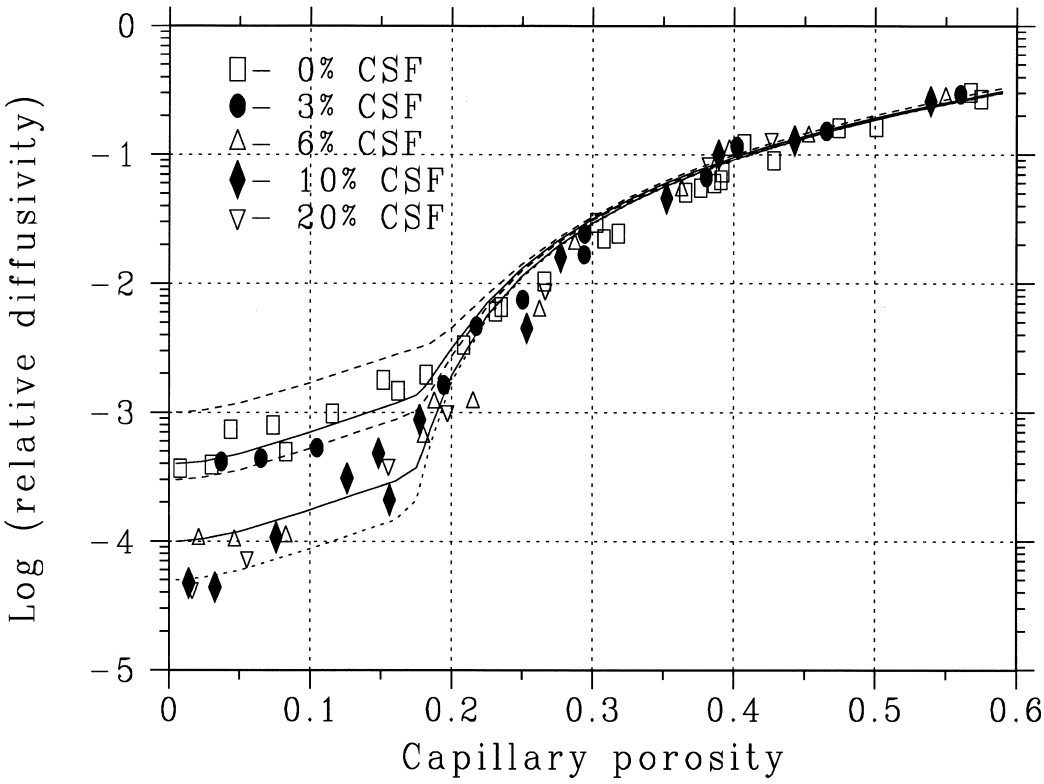

Fig. 2. Model results for relative diffusivity of cement pastes with silica fume vs. total capillary porosity. Top dashed line indicates a previously developed equation [17]. Lower four solid and dashed lines from top to bottom indicate fits for 0%, 3%, 6% and 10% silica fume additions, respectively. Fitting coefficients are provided in Table 5.

images were created matching either the Bogue composition of the cement provided above (for chloride diffusion predictions) or those provided by Delagrave et al. [20] (for tritiated water diffusion). While the exact particle size distributions of the cements were unavailable, particle size distributions from a previous study [21] that most closely matched the measured Blaine surface areas [8,20] were utilized. Silica fume was modeled as 1 pixel (1 μm^3) particles and the overall hydration volume was 100 × 100 × 100 μm or 1,000,000 pixel elements. Initial microstructures were created for the following conditions: water-to-solids ratios of 0.45 and 0.25 (with 0% and 6% silica fume replacement of cement by mass), a w/c ratio of 0.3 (with 0%, 3%, 6%, 10% and 20% silica fume additions to cement by mass), and a w/c ratio of 0.2 (with no silica fume). Hydration of the initial microstructures was then simulated at 20°C until matching the measured degree of hydration for comparison to the chloride ion diffusivity data [22] and to one set of tritiated water diffusivity data [23], and for 1000 cycles of hydration at 23°C for comparison to the tritiated water diffusivity data obtained from specimens which were cured for 3 months [20]. Relative diffusivities were then computed using an electrical analogy [17] and a previously developed and documented finite difference computer code [24]. Relative diffusivity is the ratio of the diffusivity of the diffusing species in the cement paste relative to its value when diffusing in bulk water (i.e., the inverse of the previously defined formation factor).

Two schools of thought exist concerning the pozzolanic reaction of silica fume within cement-based materials. If a global equilibrium is maintained, the silica fume should first react with all of the CH, and only when all of the CH is consumed, will the Ca/Si ratio of the C-S-H be reduced from its "average" value of 1.5–1.7 [25]. In the "local equilibrium" model, formation of a low Ca/Si ratio (e.g., 1.1) pozzolanic C-S-H occurs near the silica fume particles, while some CH may persist (albeit metastably) in locations "far" from any of the silica fume. The differences between these two models are summarized in Table 2. Based on the results of Sellevold et al. [9] and Lu et al. [10], we have chosen to implement the latter model in the NIST cement hydration and microstructure development model. Specifically, for the reaction of silica fume with CH and conventional $C_{1.7}SH_{4.0}$ gel, the following reactions are assumed in the model:

$$1.1CH + S + 2.8H \rightarrow C_{1.1}SH_{3.9}$$

$$C_{1.7}SH_{4.0} + 0.5H \rightarrow C_{1.1}SH_{3.9} + 0.6CH$$

with an assumed molar volume of 101.8 cm^3/mol for the pozzolanic $C_{1.1}SH_{3.9}$ gel [26]. Lu et al. [10] have observed that for a w/c = 0.21 (18% silica fume addition) cement

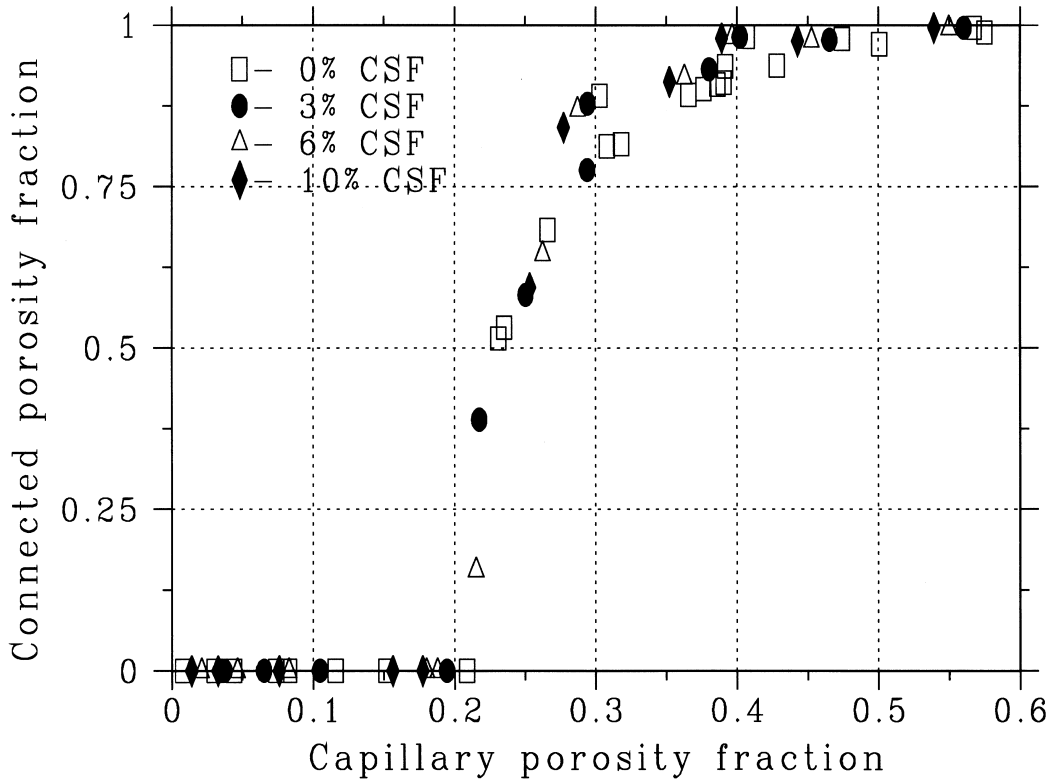

Fig. 3. Model percolation results for capillary porosity phase.

paste, the H/S molar ratio of the C-S-H decreases from 3.9 at 3 days to 2.1 at 28 days, but as a simplification, we shall here assume a constant ratio of 3.9 in the hydration model. This model with a constant H/S ratio has previously been successfully applied to predicting the adiabatic temperature rise in concretes containing silica fume [26].

It should be noted that both of these pozzolanic reactions will contribute to a further reduction in the capillary porosity of cement pastes containing silica fume due to their consumption of capillary pore water. In the NIST model, the first reaction is assumed to occur at the silica fume particle surfaces when a diffusing CH species collides with a silica fume pixel [26]. Further, the conversion of conventional C-S-H to pozzolanic C-S-H shown in the second reaction is prohibited when the unreacted silica fume content falls below 1.3% of the overall system volume. This cutoff value was selected to provide the best agreement with the experimentally measured chloride ion diffusivity for the w/c = 0.3 system with a 3% silica fume addition. For the 6% and higher silica fume additions, this criterion is never reached as the silica fume remaining after "complete" hydration always exceeds the 1.3% volume fraction. For the 0.3 w/c ratio simulated systems, and for all four different silica fume addition levels, approximately 50% of the initial silica fume reacted during the first 976 model cycles of hydration (corresponding to the measured degree of cement hydration for the w/c = 0.3, 0% silica fume specimen, 0.71). This is in general agreement with the experimental results of Lu et al. [10], who measured degrees of reaction of silica fume on the order of 45% for w/c = (0.18–0.3) cement pastes with silica fume additions between 6% and 48% hydrated for 60 days, and also observed the degree of reaction of the silica fume to be independent of silica fume content.

5. Results and discussion

5.1. Comparison of experimental and computer model data

For the tritiated water diffusion studies, the conventional C-S-H was assigned a relative diffusivity of 0.0025 (as used previously [17]) and the pozzolanic C-S-H a value of 0.0005 (five times lower, as suggested by the nanostructural models). In all simulations, the capillary porosity was assigned a relative diffusivity of 1.0. All model relative diffusivity values were then converted to absolute values by multiplying by the diffusivity of tritiated water in bulk water at 23°C, D_{HTO}, taken to be 2.24×10^{-9} m^2/s [27]. In this series of tests [20], silica fume replaced 6% of the cement on a mass basis, and diffusion coefficients were determined from a steady-state experiment.

A comparison of the simulated values and those measured experimentally is provided in Table 3. For the systems without silica fume, the model values are within 25% of the

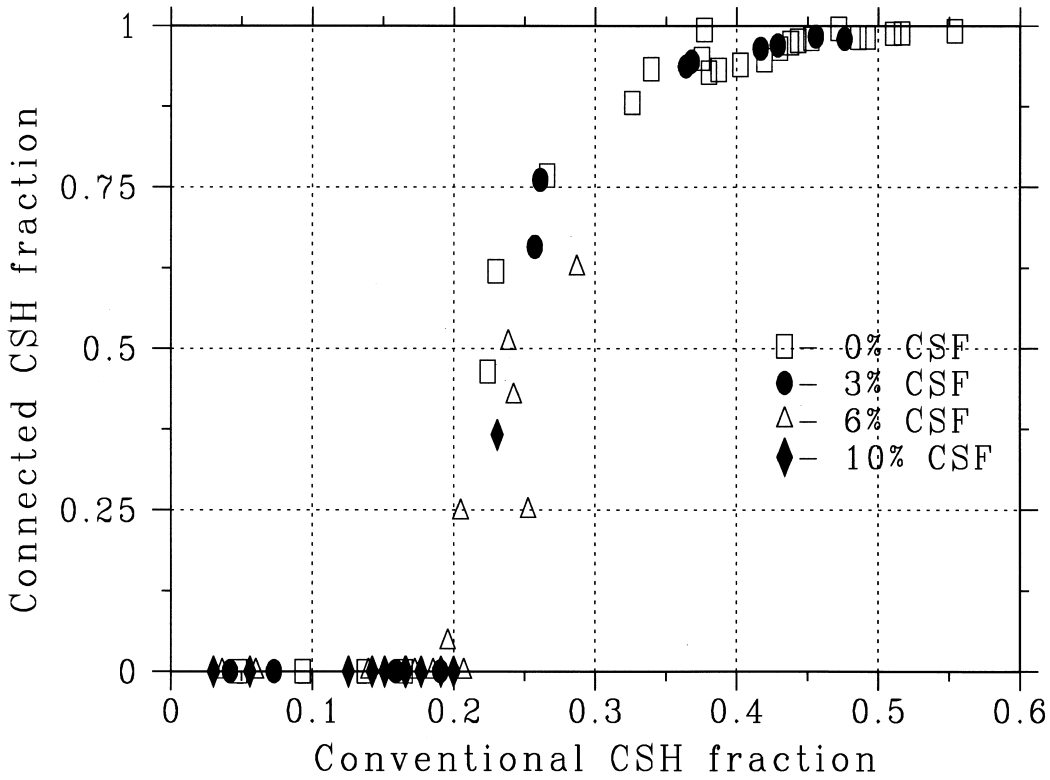

Fig. 4. Model percolation results for the conventional C-S-H phase. Note that for the 6% and 10% CSF additions, none of the data points lie to the right of the 0.3 volume fraction line.

experimental ones measured by Delagrave et al. [20], a good agreement. The model value for the 0.2 w/c ratio cement paste of Matte and Moranville [23] is about half of the measured value. Two possible reasons for this discrepancy are the 2-day 90°C curing regime applied to the experimental specimen and that the tritiated water diffusion test may have been conducted using solutions that were not saturated with respect to calcium hydroxide [23] (so that some leaching may have occurred during the measurement) unlike the tests performed by Delagrave et al. [20]. Both of these effects would tend to coarsen the pore structure, increasing the relative diffusivity of the specimen in accordance with the observed value relative to the model prediction. For the systems with 6% silica fume replacement [20], the model values are within a factor of two of the experimental ones, a reasonable agreement.

For chloride ion diffusion (assuming a diffusivity of 1.81×10^{-9} m^2/s for chloride ions in bulk water at 20°C [8]), good agreement with the experimental unleached diffusion data of Jensen [22] determined under unsteady-state conditions could only be obtained when the pozzolanic C-S-H was assigned a relative diffusivity of 0.0001 (25 times less than that of the conventional C-S-H). Once this value was used, however, as can be seen in Table 4, excellent agreement was observed between the experimental and computer model values for silica fume additions up to 10%. For the 20% silica fume addition, however, the experimental value was still far below the model value, perhaps suggesting further modification (densification) of the C-S-H nanostructure at very high levels of silica fume addition. An alternative possibility would be a further reduction in the diffusion coefficient due to the presence of unsaturated capillary porosity, despite the efforts to maintain saturation of the sample. The fact that the hydrated model system in this case has a capillary porosity of less than 2%, however, would suggest that this possibility is quite remote.

5.2. Model-based interpretation of the influence of silica fume on diffusivity

Previously, Garboczi and Bentz [17] have shown that the relative diffusivity of cement paste should be mainly a function of capillary porosity. At higher porosities (>20%), transport is dominated by the percolated pathways through the capillary porosity phase. At lower porosities (<20%), the capillary porosity becomes discontinuous and transport is controlled by the properties of the nanoporous C-S-H phase. Plotting relative diffusivity vs. total capillary porosity resulted in a single universal curve for a variety of w/c ratios and degrees of hydration [17], albeit with abrupt changes in slope at the percolation threshold porosity, for model tricalcium silicate cement pastes.

Accepting that the NIST cement hydration and microstructure development model is producing reasonable mi-

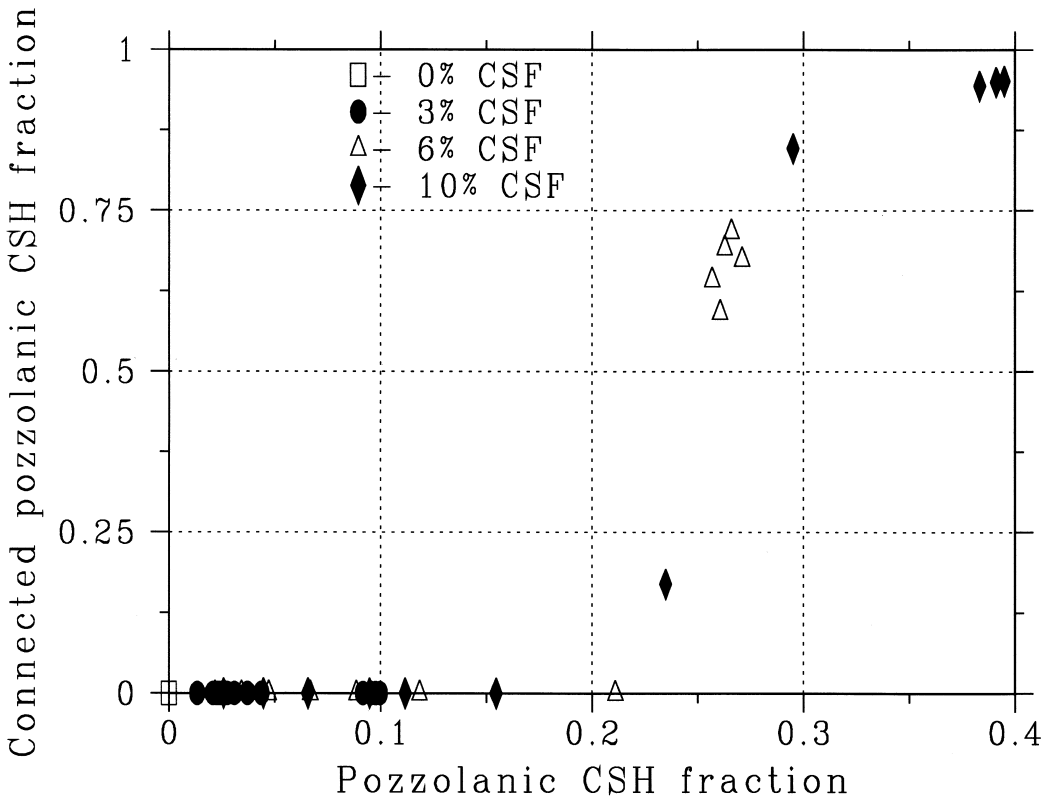

Fig. 5. Model percolation results for the pozzolanic C-S-H phase. Sufficient volume of the pozzolanic C-S-H to achieve percolation is produced only for the CSF addition rates of 6% and 10%.

crostructures and chloride ion diffusivities for systems containing silica fume, one can proceed to investigate the effects of w/c ratio, silica fume addition, and degree of hydration on relative diffusivity. For this study, approximately 70 different microstructures were simulated with w/c ratios ranging from 0.2 to 0.7 and silica fume additions from 0% to 20%. The results are summarized in Fig. 2, which provides a plot of the model relative diffusivities vs. total capillary porosity. It should be noted that the general trends of these curves are in good agreement with the experimental data for chloride ion diffusivity under leaching conditions presented by Jensen et al. [8], and the relative electrical conductivity data presented by Christensen [28] for w/c = 0.4 cement pastes with (20%) and without silica fume.

At high porosities, the data collapse onto a single curve as the capillary porosity and its connectivity regulates the ease of transport. As the capillary porosity depercolates at about 20% porosity, however, the curves diverge into individual curves for the different silica fume contents. Once the capillary pore space is disconnected, transport will be regulated by the percolation of the conventional C-S-H and the pozzolanic C-S-H. The percolation properties of each of these three phases, assessed using a pixel-based burning algorithm [29], are provided in Figs. 3–5. Each phase is observed to exhibit a percolation threshold somewhere between 20% and 30% volume fraction, the connectivity of the capillary porosity strictly decreasing and that of the pozzolanic C-S-H strictly increasing with advancing hydration (when sufficient pozzolan is present). The progress of the percolation of the conventional C-S-H with advancing hydration is more complicated, as discussed below.

In the systems with low (0% and 3%) silica fume additions, from Fig. 4, the conventional C-S-H is seen to be highly percolated for C-S-H volume fractions greater than 0.30 and its relative diffusivity (0.0025) will control the overall diffusivity once the capillary porosity becomes discontinuous. For the systems with higher (6% and 10%) silica fume additions, the conventional C-S-H begins to percolate somewhat, but never exceeds a volume fraction of 0.3 due to the "slow" ongoing conversion of conventional C-S-H into pozzolanic C-S-H via the second chemical reaction presented earlier. This behavior can be seen more clearly in Fig. 6, which plots the conventional C-S-H volume fraction vs. the capillary porosity fraction for various w/c ratios and CSF addition rates. The plot is conveniently divided into four quadrants indicated by the two solid lines parallel to the x and y axes. In the lower right quadrant, the capillary porosity is percolated and the conventional C-S-H is discontinuous. In the upper right quadrant, both phases are percolated. In the upper left quadrant, the capillary porosity is discontinuous while the conven-

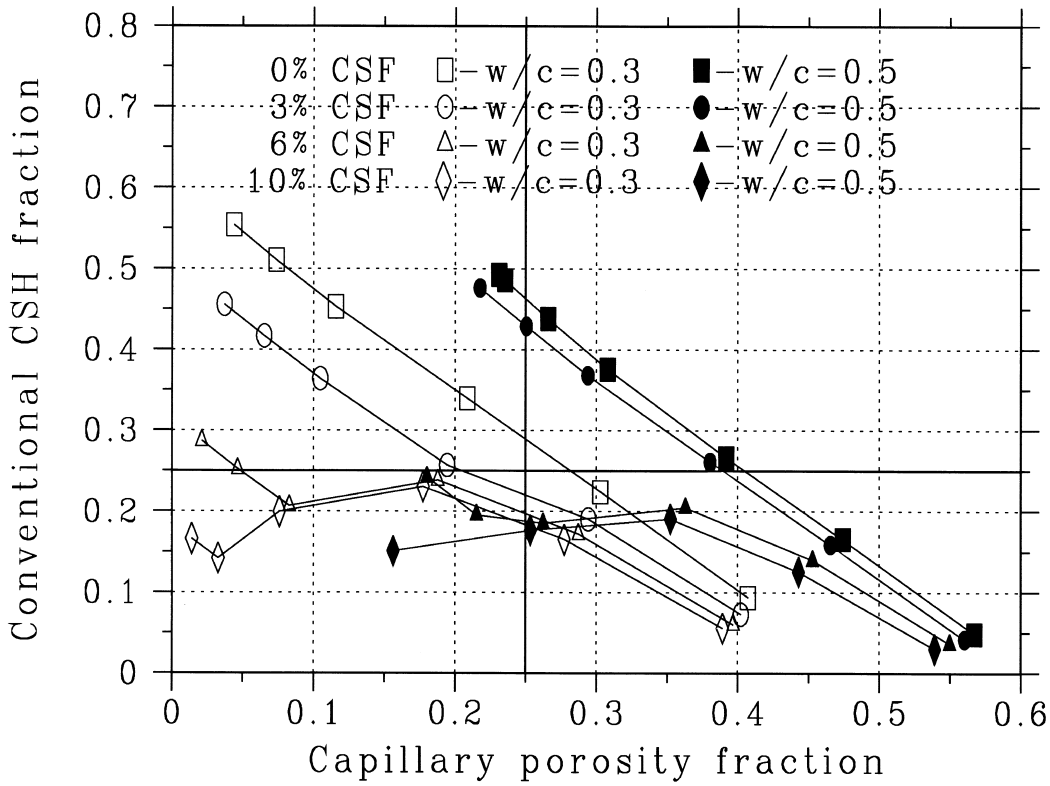

Fig. 6. Conventional C-S-H volume fraction vs. capillary porosity for various w/c ratios and CSF additions rates. As time increases, capillary porosity strictly decreases, so time is advancing as each curve proceeds from right to left in the graph. Solid lines parallel to y and x axes indicate the approximate percolation thresholds (50% connected) for the capillary porosity and the conventional C-S-H, respectively.

tional C-S-H is percolated. Finally, in the lower left quadrant, both the capillary porosity and the conventional C-S-H are discontinuous and transport would be controlled by the remaining porous and percolated phase, the pozzolanic C-S-H. In Fig. 6, in every case, as the hydration proceeds, the capillary porosity is strictly decreasing, so that each curve in Fig. 6 proceeds from right to left as time advances. For the 0% and 3% silica fume additions, the conventional C-S-H fraction is basically linearly increasing with a decrease in porosity. Thus, as hydration proceeds, the capillary porosity disconnects, while the C-S-H becomes highly percolated. However, for the 6% and 10% additions, the curves are seen to first increase, but plateau around 15% to 25% conventional C-S-H volume fraction and end up in the lower left quadrant of the plot, due to the conversion of the conventional C-S-H to pozzolanic C-S-H. Thus, for these systems, it is the pozzolanic C-S-H that becomes highly connected at long hydration times (Fig. 5) and will dominate the overall transport rates.

Previously, Garboczi and Bentz [17] developed an equation to relate relative diffusivity, D/D_0, to capillary porosity, ϕ, of the form Eq. (1):

$$\frac{D}{D_0}(\phi) = K_1 + K_2\phi^2 + K_3(\phi - \phi_c)^2 H(\phi - \phi_c) \qquad (1)$$

where K_1, K_2, and K_3 are fitting coefficients, ϕ_c represents the capillary porosity percolation threshold, and H is the Heaviside function ($H(x) = 1$ when $x > 0$ and 0 otherwise). This equation was fitted to the data available for each silica fume addition and the resulting coefficients are provided in Table 5. In agreement with the above discussion, one finds that K_3 is independent of silica fume addition, as this coefficient represents the contribution of the percolated capillary porosity to the overall diffusivity. K_1 and K_2 are seen to vary with silica fume content, but in a similar fashion. Thus, one may write Eq. (2):

$$\frac{D}{D_0}(\phi, \mathrm{CSF}) = \frac{K_1'}{\beta(\mathrm{CSF})} + \frac{K_2'}{\beta(\mathrm{CSF})}\phi^2 + K_3' \times (\phi - 0.17)^2 H(\phi - 0.17) \qquad (2)$$

where $K_1' = 0.0004$, $K_2' = 0.03$, $K_3' = 1.7$, and β is a function of silica fume addition, according to the values provided in Table 5.

The value for β for a 10% silica fume addition in Table 5 predicts an eight-fold reduction in chloride ion diffusivity for mature specimens hydrated to equal porosities. However, the actual experimental and model data provided in Table 4 indicate a 17–28-fold reduction in diffusivity. The apparent difference in these two reduction factors is due to the fact that the data values in Table 4 were obtained at equal hydration times and not at equivalent capillary porosities. Because the pozzolanic reactions con-

Table 5
Coefficients for fitting Eq. (1) to model data with $\phi_c = 0.17$

% CSF addition	K_1	K_2	K_3	β
0	0.0004	0.03	1.7	1.0
3	0.0003	0.0225	1.7	1.33
6	0.0001	0.0075	1.7	4.0
10	0.00005	0.00375	1.7	8.0

tribute to a more efficient reduction of capillary porosity than cement hydration by itself (as can be witnessed by the additional water consumed in the presented pozzolanic reactions), at equal ages, the reduction in diffusivity in samples containing silica fume additions is due both to a reduction in capillary porosity and to a reduction in the inherent diffusivity of the C-S-H. The reduction in capillary porosity at equal hydration times (cycles) can also be observed by comparing the leftmost data points for each curve in Fig. 6. For the w/c = 0.3 systems, for example, the "final" (2000 cycles of hydration) capillary porosity fractions are approximately 0.044 and 0.014 for the 0% and 10% CSF additions, respectively. For the corresponding w/c = 0.5 systems, the reduction after 2400 cycles of hydration is from 0.235 to 0.156.

Silica fume is also known to accelerate the early hydration reactions, but this is likely not a major factor for mature specimens of the lower w/c ratios generally characterizing high performance concretes, as the ultimate degree of hydration of the *cement* will be less in the systems containing silica fume due to space (capillary porosity) limitations. A further consideration in concrete is the improvement in the microstructure of the interfacial transition zone provided by the addition of silica fume [30]. In part II of this paper, a suite of multi-scale models incorporating all of these various influences will be applied in developing an equation to predict the chloride ion diffusivity of a concrete as a function of w/c ratio, silica fume addition, degree of hydration and volume fraction of aggregates. However, suffice it to say that the addition of silica fume may (when cracking due to self-desiccation and thermal gradients is avoided or minimized) dramatically increase the service life of a steel-reinforced concrete exposed to chloride ions, resulting in substantial cost savings when a life cycle costing approach [31] is applied to concrete construction.

6. Conclusions

Experimental and computer simulation studies have provided a clearer understanding of the role of silica fume in reducing the diffusivity of cement-based materials. The results are consistent with an inherent reduction in the diffusivity of the pozzolanic C-S-H relative to that of the conventional C-S-H. The reduction appears to be on the order of a factor of five for the diffusion of tritiated water and a factor of 25 for the diffusion of chloride ions. The microstructural models suggest that in systems containing silica fume, at high (>20%) capillary porosities, the diffusivity is regulated by the percolated capillary pore network, while at low (<20%) capillary porosities, it is controlled by the volume fractions and percolation characteristics of the two types of C-S-H.

Considering the reduced capillary porosity present at equal degrees of cement hydration in the systems containing silica fume, along with the change in the nanostructure and diffusivity of the C-S-H, after equal hydration times, a 10% addition of silica fume could result in a chloride ion diffusivity more than 15 times less than that in a comparable concrete made without silica fume. While the tendency of silica fume to detrimentally reduce the chloride threshold necessary to initiate corrosion must also be considered, in certain circumstances, this reduction in diffusivity should translate directly into a 15-fold increase in the service life of the exposed concrete, resulting in substantial life cycle cost savings for concrete construction.

Acknowledgments

Dale Bentz would like to thank the Technical University of Denmark and the Knud Hojgaard Foundation for funding a 3-month visit in support of this research and the Partnership for High Performance Concrete Technology (PHPCT) program at NIST for partial funding of this research. The Engineering and Physical Science Research Council (UK) funded the electron microprobe.

References

[1] D.P. Bentz, Three-dimensional computer simulation of cement hydration and microstructure development, J Am Ceram Soc 80 (1) (1997) 3–21.
[2] O.M. Jensen, P.F. Hansen, Autogenous deformation and change of the relative humidity in silica fume-modified cement paste, ACI Mater J 93 (6) (1996) 539–543.
[3] J. Baron, H. Van Damme, Betons: La nouvelle frontiere est au niveau moleculaire, Rev Fr Genie Civ 2 (4) (1998) 407–415.
[4] R.D. Hooton, P. Pun, T. Kojundic, P. Fidjestol, Influence of silica fume on chloride resistance of concrete, Proc. of the PCI/FHWA International Symposium on High Performance Concrete, 1997, pp. 245–256.
[5] K. Byfors, Influence of silica fume and flyash on chloride diffusion and pH values in cement paste, Cem Concr Res 17 (1987) 115–130.
[6] K. Tori, M. Kawamura, Pore structure and chloride ion permeability of mortars containing silica fume, Cem Concr Compos 16 (1994) 279–286.
[7] AASHTO T 277-83, Standard method of test for rapid determination of the chloride permeability of concrete, American Association of State Highway and Transportation Officials, Washington, DC, 1983.
[8] O.M. Jensen, P.F. Hansen, A.M. Coats, F.P. Glasser, Chloride ingress in cement paste and mortar, Cem Concr Res 29 (9) (1999) 1497–1504.
[9] E.J. Sellevold, D.H. Bager, E.K. Jensen, T. Knudsen, Silica fume

cement paste — hydration and pore structure, in: O.E. Gjorv, K.E. Loland (Eds.), Condensed Silica Fume in Concrete, Univ of Trondheim, Norway, 1982, pp. 19–50.
[10] P. Lu, G. Sun, J.F. Young, Phase composition of hydrated DSP cement pastes, J Am Ceram Soc 76 (1) (1993) 1003–1007.
[11] H.F.W. Taylor, Cement Chemistry, Thomas Telford, London, 1997.
[12] V. Baroghel-Bouny, Texture and moisture properties of ordinary and high-performance cementitious materials, Proc. of the International RILEM Conference "Concrete: from Material to Structure,"1998, pp. 144–165.
[13] T.C. Powers, T.L. Brownyard, Studies of the physical properties of hardened portland cement paste, J Am Concr Inst 43 (1947) pp. 101, 249, 469, 549, 669, 845, 993.
[14] T.C. Powers, T.L. Brownyard, Studies of the physical properties of hardened portland cement paste, PCA Bull Portland Cement Association, p. 22.
[15] D.P. Bentz, E.J. Garboczi, D.A. Quenard, V. Baroghel-Bouny, H.M. Jennings, Modelling drying shrinkage of cement paste and mortar: Part I. Structural models from nanometers to millimeters, Mater Struct 28 (1995) 450–458.
[16] A.J. Allen, R.C. Oberthur, D. Pearson, P. Scholfield, C.R. Wilding, Development of the fine porosity and gel structure of hydrating cement, Philos Mag B 56 (3) (1987) 263–288.
[17] E.J. Garboczi, D.P. Bentz, Computer simulation of the diffusivity of cement-based materials, J Mater Sci 27 (1992) 2083–2092.
[18] S. Phillipot, J.-P. Korb, D. Petit, G. Counio, H.J. Zanni, Analysis of the microporosity of reactive powder concrete by proton nuclear relaxation, Chim Phys 95 (1998) 332–336.
[19] J.-P. Korb, D. Petit, S. Philippot, H. Zanni, V. Maret, M. Cheyrezy, Nuclear relaxation of water confined in reactive powder concrete, in: P. Colombet (Ed.), Resonance Spectroscopy of Cement-based Materials, Springer-Verlag, Berlin, Germany, 1997, pp. 333–343.
[20] A. Delagrave, J. Marchand, M. Pigeon, Influence of microstructure on the tritiated water diffusivity of mortars, Adv Cem Based Mater 7 (1998) 60–65.
[21] D.P. Bentz, C.J. Haecker, An argument for using coarse cements in high performance concrete, Cem Concr Res 29 (4) (1999) 615–618.
[22] O.M. Jensen, Chloride ingress in cement paste and mortar measured by electron probe micro analysis, Technical Report, Series R, No. 51, Technical University of Denmark, 1998.
[23] V. Matte, M. Moranville, Durability of reactive powder composites: Influence of silica fume on the leaching properties of very low water/binder pastes, Cem Concr Compos 21 (1999) 1–9.
[24] E.J. Garboczi, Finite element and finite difference programs for computing the linear electric and elastic properties of digital images of random materials, NISTIR 6269, US Department of Commerce, December, 1998. (see http://ciks.cbt.nist.gov/garboczi/, Chap. 2).
[25] V.G. Papadakis, Supplementary cementing materials in concrete — activity, durability, and planning, Final Report — Project No ERBFMGICT961387, Danish Technological Institute, January, 1999.
[26] D.P. Bentz, V. Waller, F. deLarrard, Prediction of adiabatic temperature rise in conventional and high-performance concretes using a 3-D microstructural model, Cem Concr Res 28 (2) (1998) 285–297.
[27] R. Mills, V.M.M. Lobo, Self-Diffusion in Electrolyte Solutions, Elsevier, Amsterdam, 1989, p. 317.
[28] B. Christensen, Microstructural studies of hydrating portland cement-based materials using impedance spectroscopy, PhD thesis, Northwestern University, 1993.
[29] D.P. Bentz, E.J. Garboczi, Percolation of phases in a three-dimensional cement paste microstructural model, Cem Concr Res 21 (1991) 325–344.
[30] D.P. Bentz, E.J. Garboczi, Simulation studies of the effects of mineral admixtures on the cement paste–aggregate interfacial zone, ACI Mater J 88 (5) (1991) 518–529.
[31] M.A. Ehlen, BridgeLCC 1.0 Users Manual, NISTIR 6298, US Department of Commerce, 1999 April.